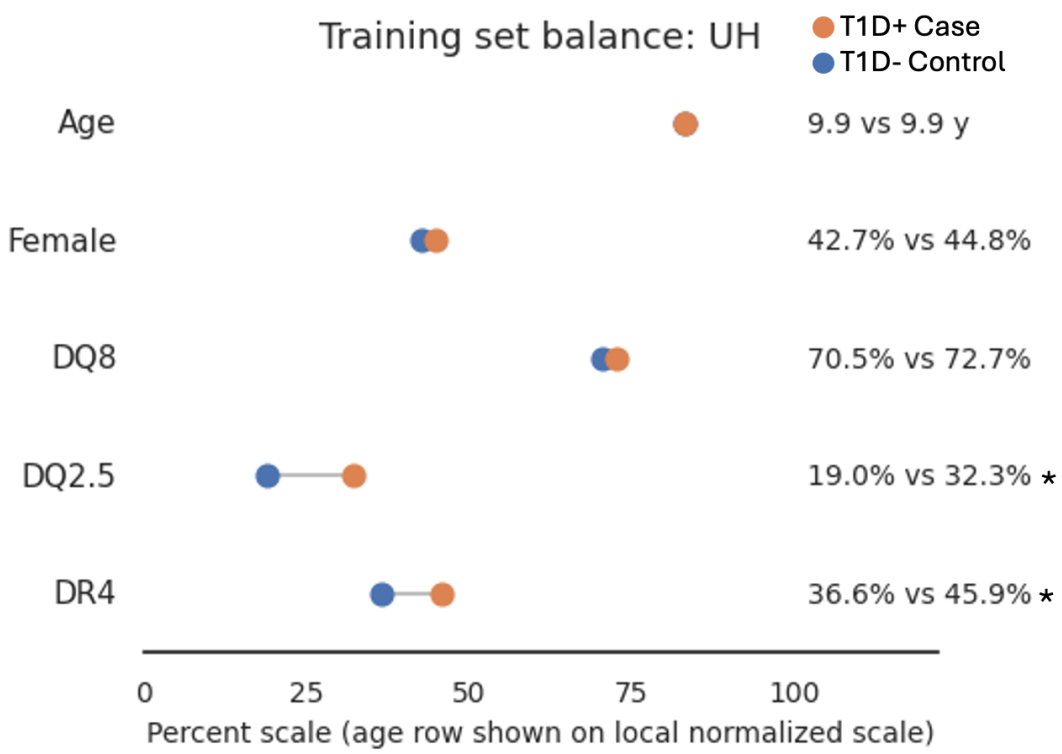


**Figure S1 | Discovery-cohort balance in the UH training set.**
Age, sex, and inferred HLA composition in the UH discovery/training set, comparing T1D cases and controls. The slide reports closely matched age and sex distributions and modest differences in DQ2.5 and DR4 frequencies. Asterisks indicate Fisher exact test $p < 0.01$ for binary variables; age was compared by Welch t test.

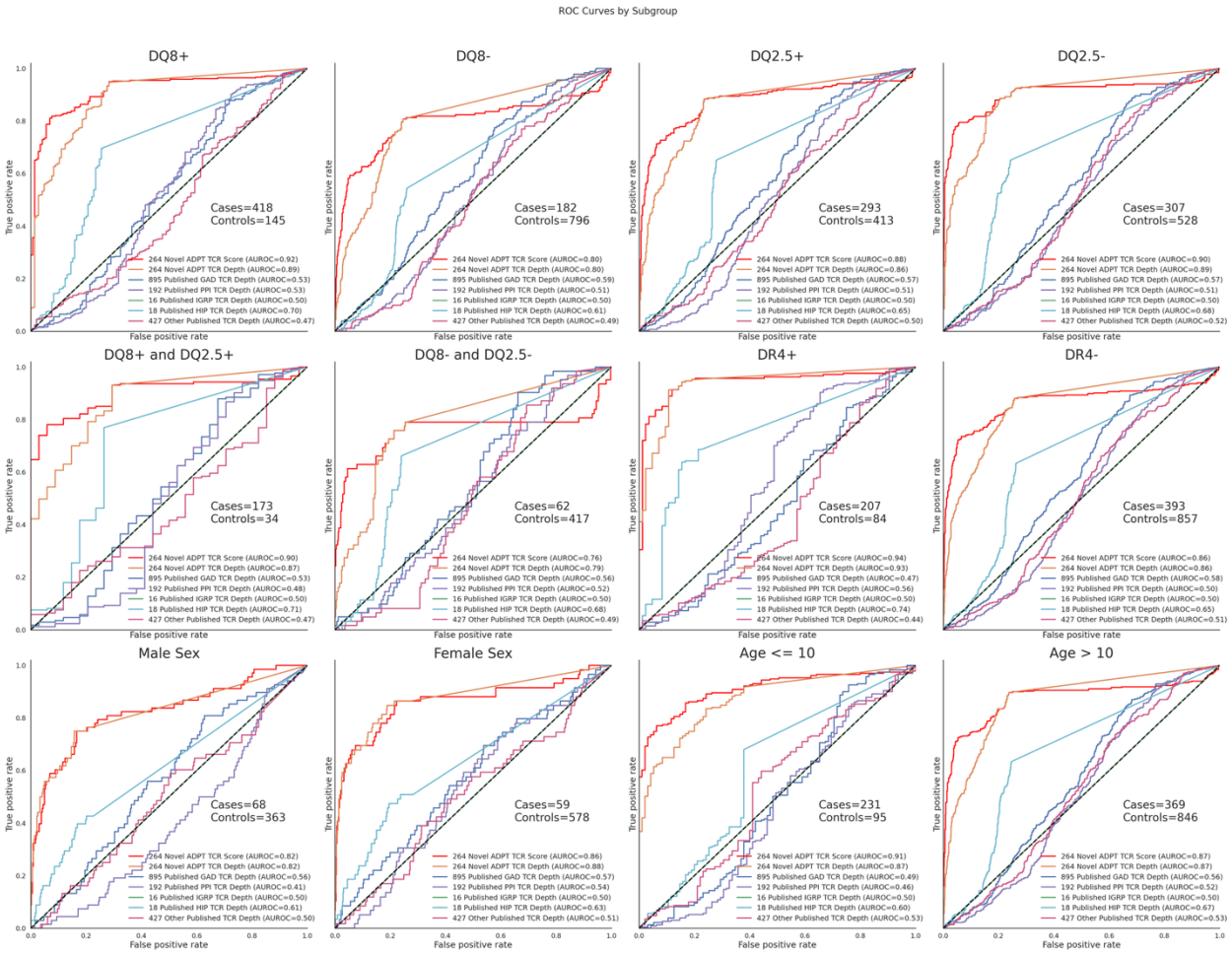


**Figure S2 | Locked-model performance across major HLA, age, and sex subgroups.**
ROC curves for the 264-receptor score, 264-receptor clonal depth, and the published comparator receptor sets within the displayed subgroups. Score AUROCs range from 0.76 in the worst performing subgroup (DQ8- and DQ2.5-) to 0.94 in the best performing subgroup (DR4+) for the 264 novel ADPT TCR model (red curve) across these subgroup analyses.

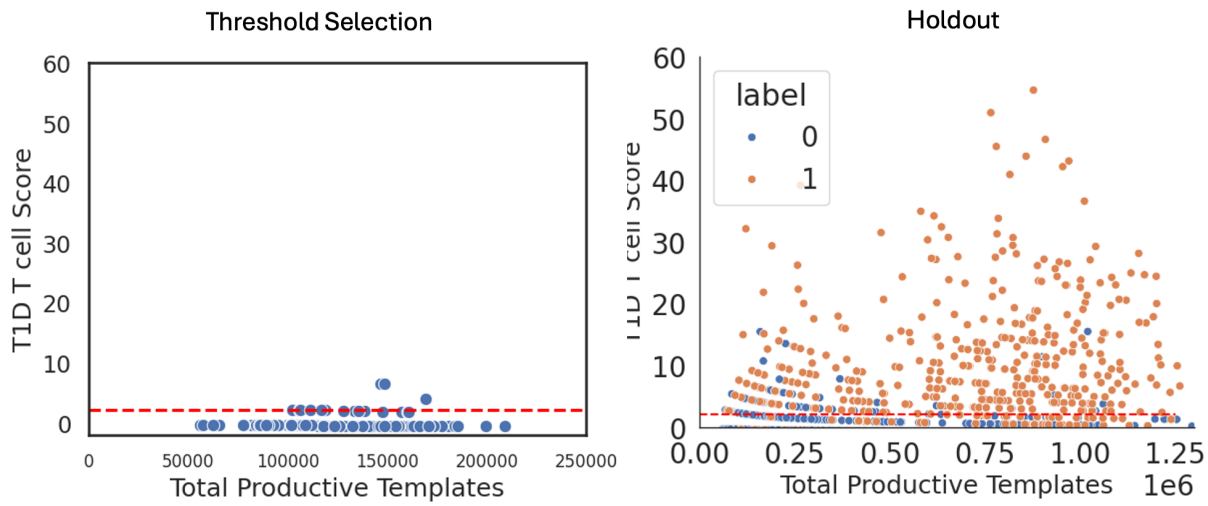


**Figure S3 | Threshold-selection and holdout score distributions relative to sequencing depth.** Scatterplots of T1D model score versus total productive templates in the UF threshold-selection controls (left) and the holdout cohort (right). The horizontal dashed line marks the locked threshold derived from UF controls (score = 2.13). The figure illustrates that the locked cutoff is defined externally to the holdout cohorts and is not obviously driven by template depth alone.

**ADPT_C1 size=62**

OR=23.79 q=1.3e-159 HLA=DQ8 (OR=5.06)

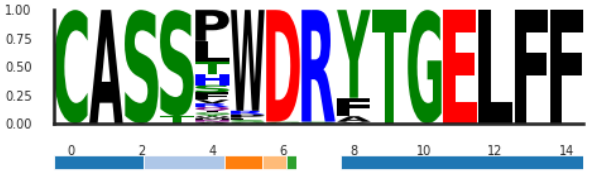

TCRBV12-01: 37.0%
TCRBV07-02: 33.0%
TCRBV11-02: 15.7%
TCRBV07-03: 10.1%
TCRBV07-07: 4.3%

TCRBJ02-02: 100.0%

**ADPT_C2 size=45**

OR=17.76 q=7.8e-163 HLA=DQ8 (OR=5.20)

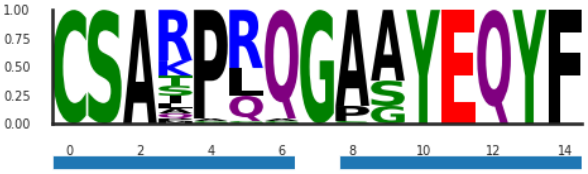

TCRBV20-01: 100.0%

TCRBJ02-07: 100.0%

**ADPT_C3 size=10**

OR=5.79 q=1.7e-55 HLA=DQ8 (OR=2.94)

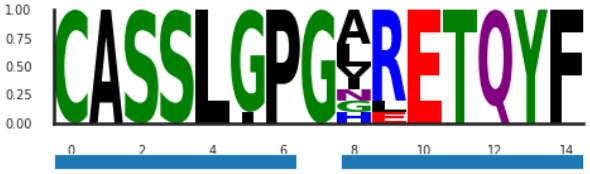

TCRBV05-01: 100.0%

TCRBJ02-05: 100.0%

**ADPT_C4 size=8**

OR=5.60 q=3.2e-47 HLA=DQ2.5 (OR=6.63)

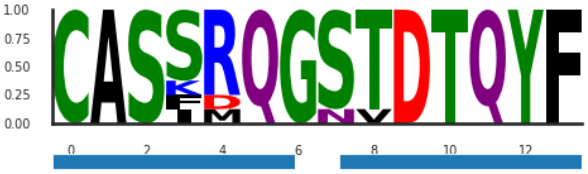

TCRBV07-09: 100.0%

TCRBJ02-03: 100.0%

**ADPT_C5 size=6**

OR=4.18 q=2.9e-56 HLA=DRB4*01:03 (OR=2.20)

TCRBV03-01/03-02: 100.0%

TCRBJ01-02: 100.0%

**ADPT_C6 size=10**

OR=17.78 q=1.3e-38 HLA=DQ8 (OR=3.37)

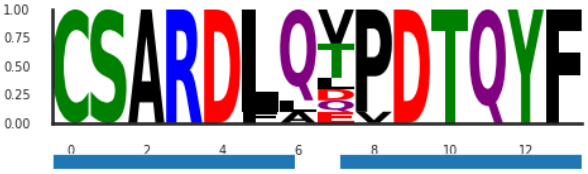

TCRBV20-01: 100.0%

TCRBJ02-03: 100.0%

**ADPT_C7 size=4**

OR=inf q=1.1e-30 HLA=DQ8 (OR=7.10)

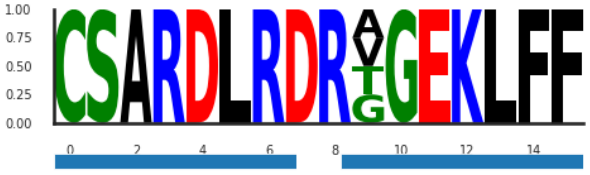

TCRBV20-01: 100.0%

TCRBJ01-04: 100.0%

**ADPT_C9 size=8**

OR=9.56 q=2.4e-20 HLA=DQ2.5 (OR=2.65)

TCRBV20-01: 100.0%

TCRBJ02-07: 100.0%

**ADPT_C10 size=7**

OR=26.49 q=3.2e-15 HLA=DQ8 (OR=2.83)

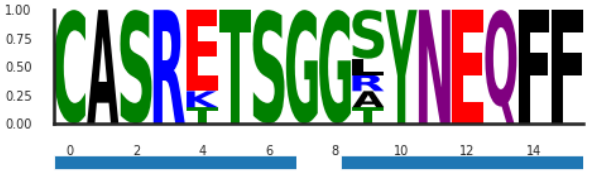

TCRBV06-06: 100.0% TCRBJ02-01: 100.0%

**ADPT_C11 size=7**

OR=7.39 q=1.2e-14 HLA=DQ8 (OR=2.24)

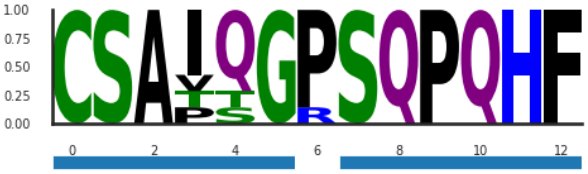

TCRBV20-01: 100.0% TCRBJ01-05: 100.0%

**ADPT_C12 size=7**

OR=15.25 q=4.3e-19 HLA=DQ8 (OR=3.11)

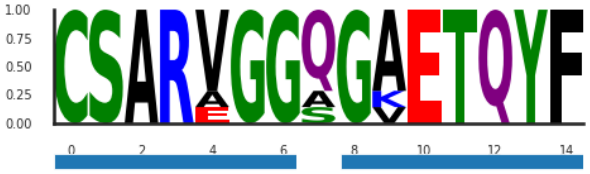

TCRBV20-01: 100.0% TCRBJ02-05: 100.0%

**ADPT_C13 size=6**

OR=78.59 q=2.6e-24 HLA=DQ8 (OR=6.50)

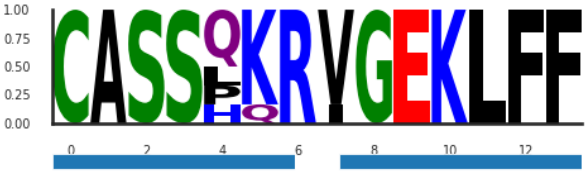

TCRBV03-01/03-02: 100.0% TCRBJ01-04: 100.0%

**ADPT_C14 size=5**

OR=18.82 q=3.2e-15 HLA=DQ5 (OR=14.32)

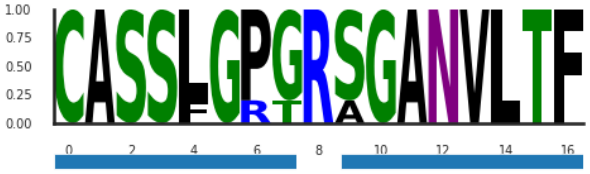

TCRBV05-06: 100.0% TCRBJ02-06: 100.0%

**ADPT_C15 size=5**

OR=9.24 q=5.8e-23 HLA=DQ8 (OR=2.03)

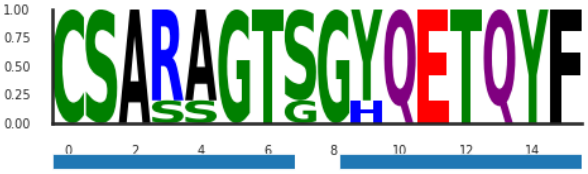

TCRBV20-01: 100.0% TCRBJ02-05: 100.0%

**ADPT_C16 size=5**

OR=14.25 q=6.4e-36 HLA=DQ8 (OR=3.64)

TCRBV20-01: 100.0% TCRBJ01-01: 100.0%

**ADPT_C17 size=4**

OR=10.43 q=1.1e-24 HLA=DQ8 (OR=1.89)

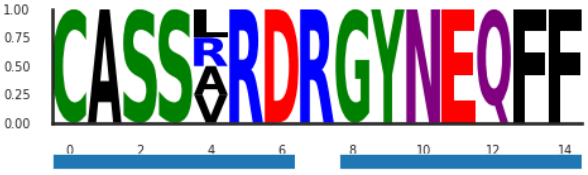

TCRBV04-02: 100.0% TCRBJ02-01: 100.0%

**ADPT_C18 size=4**

OR=5.71 q=1.9e-09 HLA=DQ5 (OR=6.69)

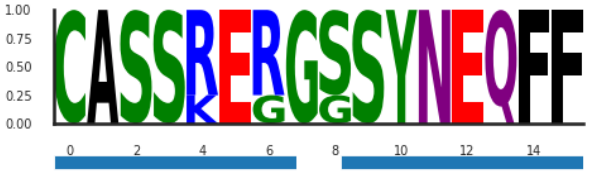

TCRBV05-01: 100.0% TCRBJ02-01: 100.0%

**ADPT_C19 size=4**

OR=9.92 q=3.2e-34 HLA=DQ8 (OR=2.62)

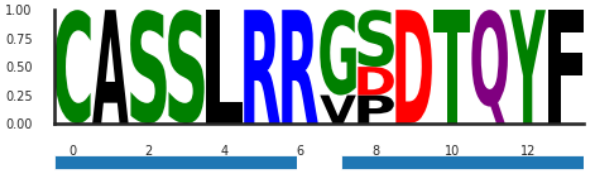

TCRBV05-01: 100.0% TCRBJ02-03: 100.0%

**ADPT_C20 size=4**

OR=10.56 q=1.2e-14 HLA=nan (OR=1.82)

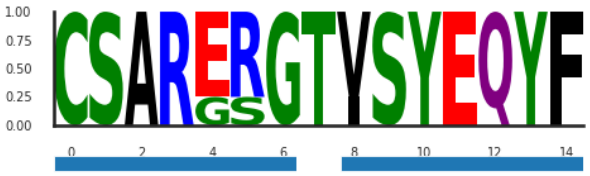

TCRBV20-01: 100.0% TCRBJ02-07: 100.0%

**ADPT_C21 size=4**

OR=11.40 q=2.8e-25 HLA=DQ8 (OR=4.28)

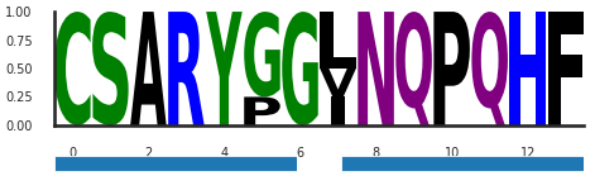

TCRBV20-01: 100.0% TCRBJ01-05: 100.0%

**ADPT_C22 size=2**

OR=21.27 q=4.0e-12 HLA=DQ8 (OR=2.85)

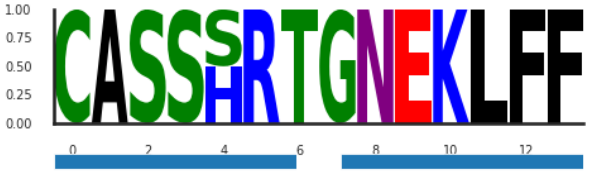

TCRBV04-02: 100.0% TCRBJ01-04: 100.0%

**ADPT_C23 size=2**

OR=14.45 q=1.1e-14 HLA=DQ5 (OR=13.88)

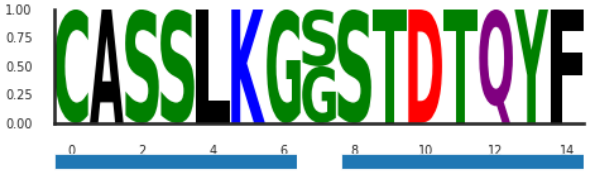

TCRBV11-03: 100.0% TCRBJ02-03: 100.0%

**ADPT_C24 size=2**

OR=13.38 q=2.2e-07 HLA=DQ8 (OR=4.67)

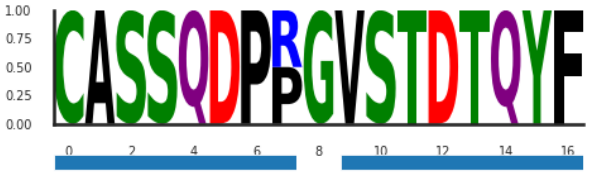

TCRBV04-02: 100.0% TCRBJ02-03: 100.0%

**ADPT_C25 size=1**

OR=3.27 q=1.3e-04 HLA=nan (OR=5.29)

TCRBV06-04: 100.0% TCRBJ01-01: 100.0%


**Figure S4 | Extended logo gallery of disease-associated public TCR clusters.**
Additional sequence logos for disease-associated public clusters beyond the top five shown in Fig. 2. Each panel displays cluster size, case-enrichment odds ratio, q value, the dominant HLA association, and dominant V/J usage where applicable.

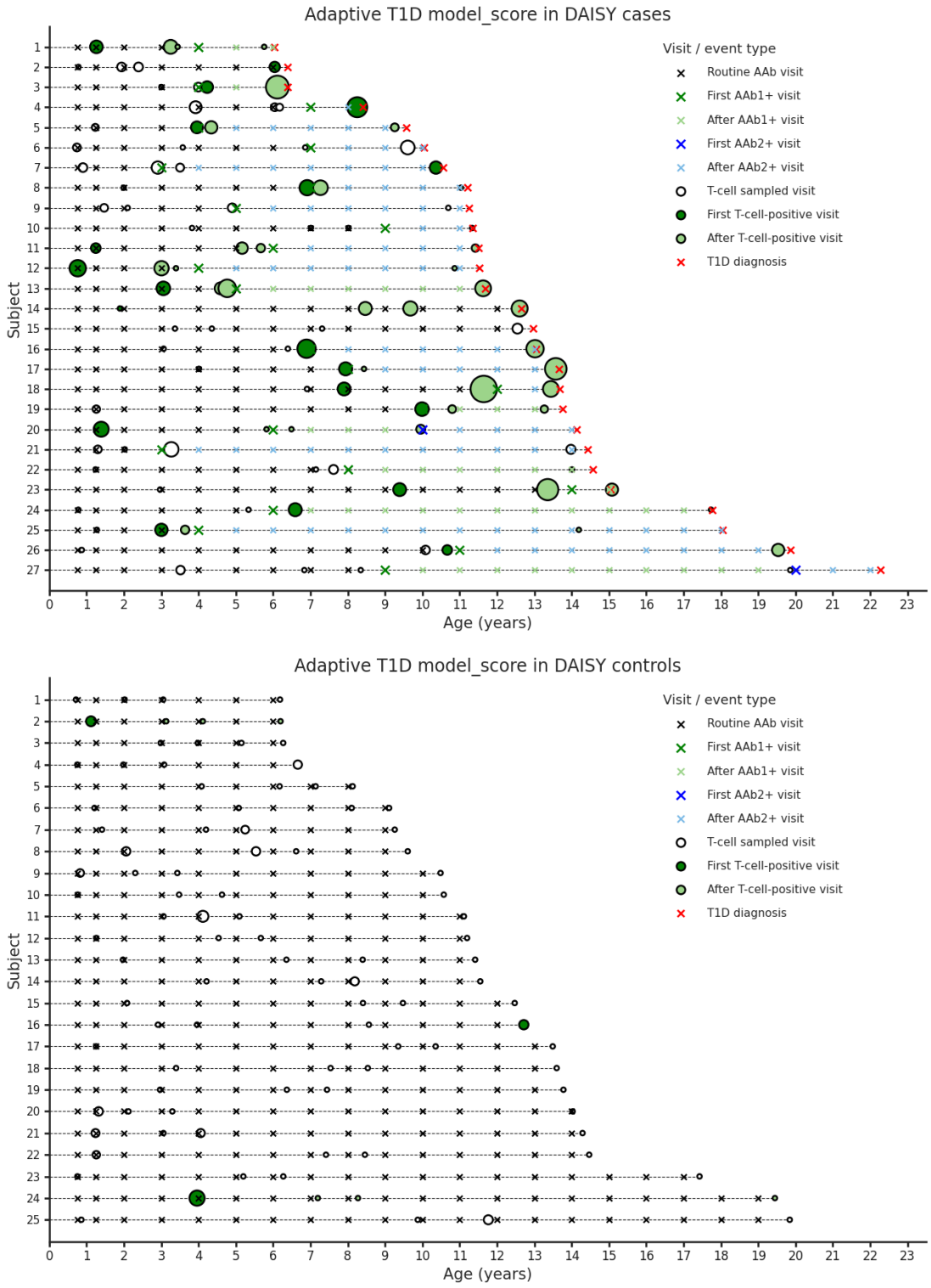


**Figure S5 | Full timeline for TCR and AAb sampling for DAISY cohort**

Donors who eventually develop T1D (cases) are show on the top panel and donors who don't progress to T1D (controls) are shown on the bottom panel. Size of circle indicates magnitude of T cell-based model score. Dark green indicates first T-cell or Aab positive timepoint, light green indicates later positive timepoints. Red x indicates T1D diagnosis.

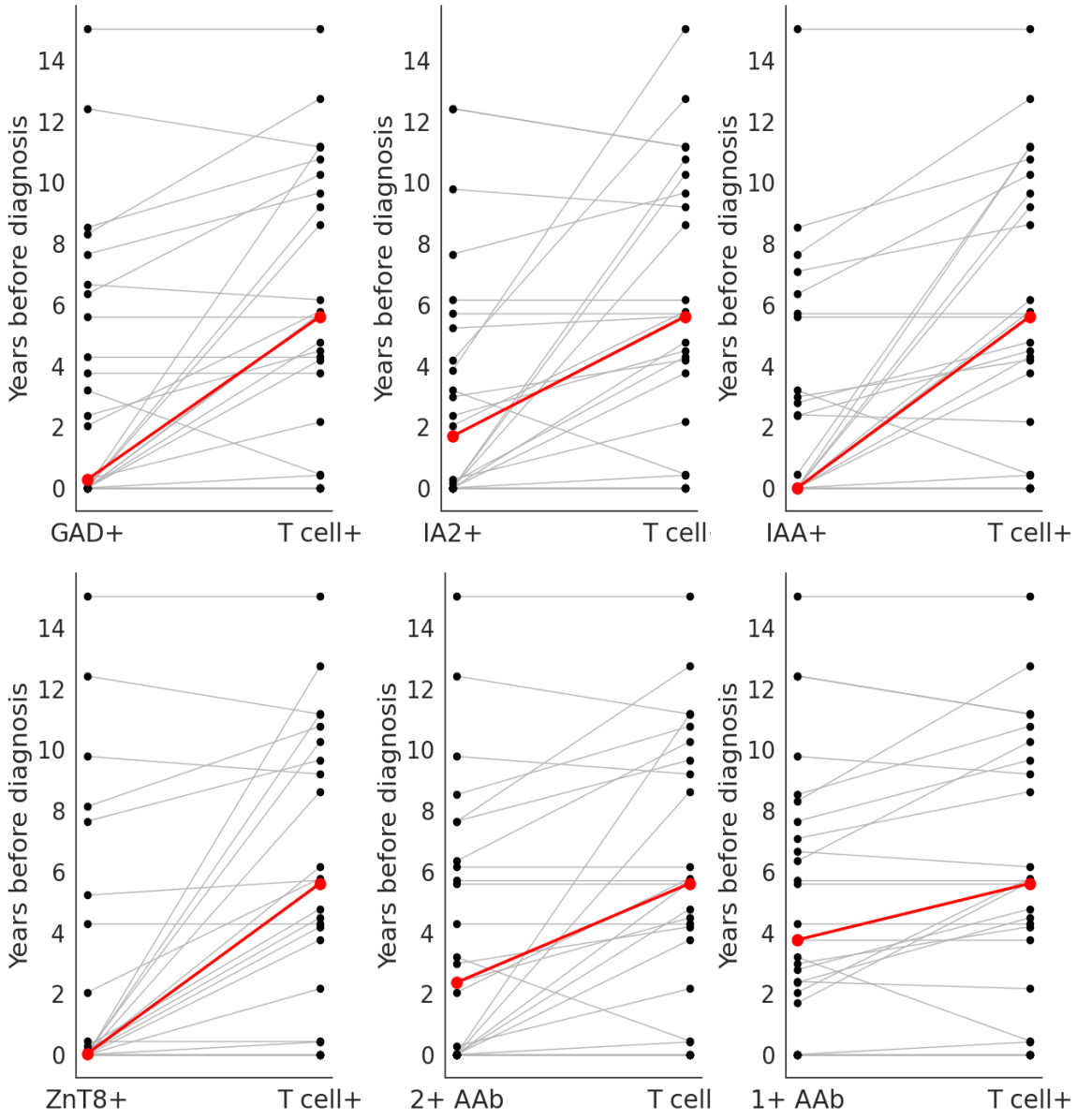


**Figure S6 | Paired DAISY timing comparisons for individual serologic milestones.**
Within-participant paired plots of years before diagnosis for GAD+, IA-2+, IAA+, ZnT8+, 2+ autoantibodies, and 1+ autoantibodies versus first T-cell positivity. Red markers denote the group means shown in the plotted panel. Across all six comparisons, T-cell positivity tends to occur earlier than the matched serologic milestone in the paired subset used for these plots.

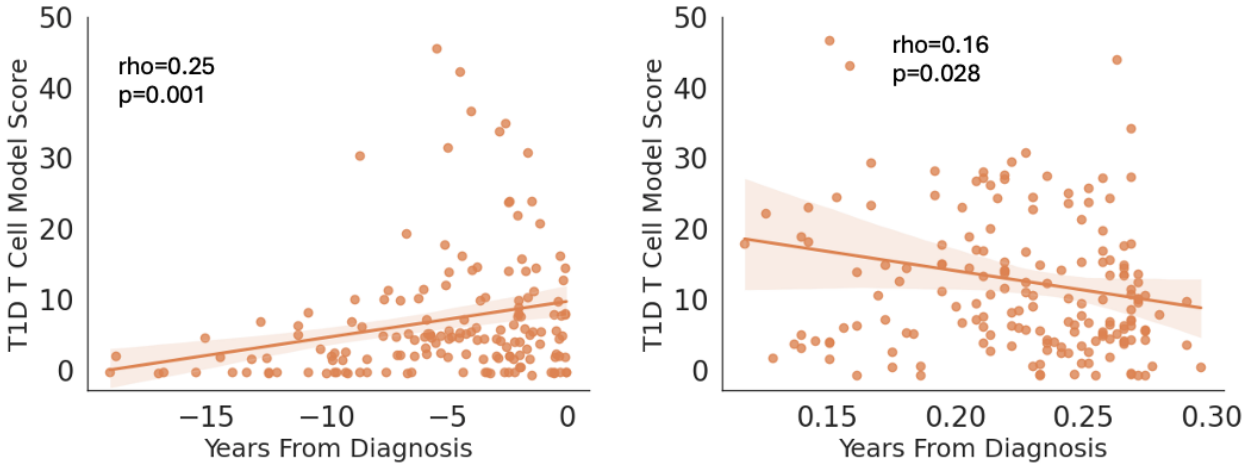


**Figure S7 | Relationship between T-cell model score and time from diagnosis.**
Left, correlation between model score and years before diagnosis in prediagnosis samples (Spearman rho = 0.25, p = 0.001). Right, correlation between model score and years from diagnosis in the early postdiagnosis window displayed in the panel (Spearman rho = 0.16, p = 0.028). These plots support a rise in the biomarker approaching diagnosis and a weaker inverse trend shortly after diagnosis.

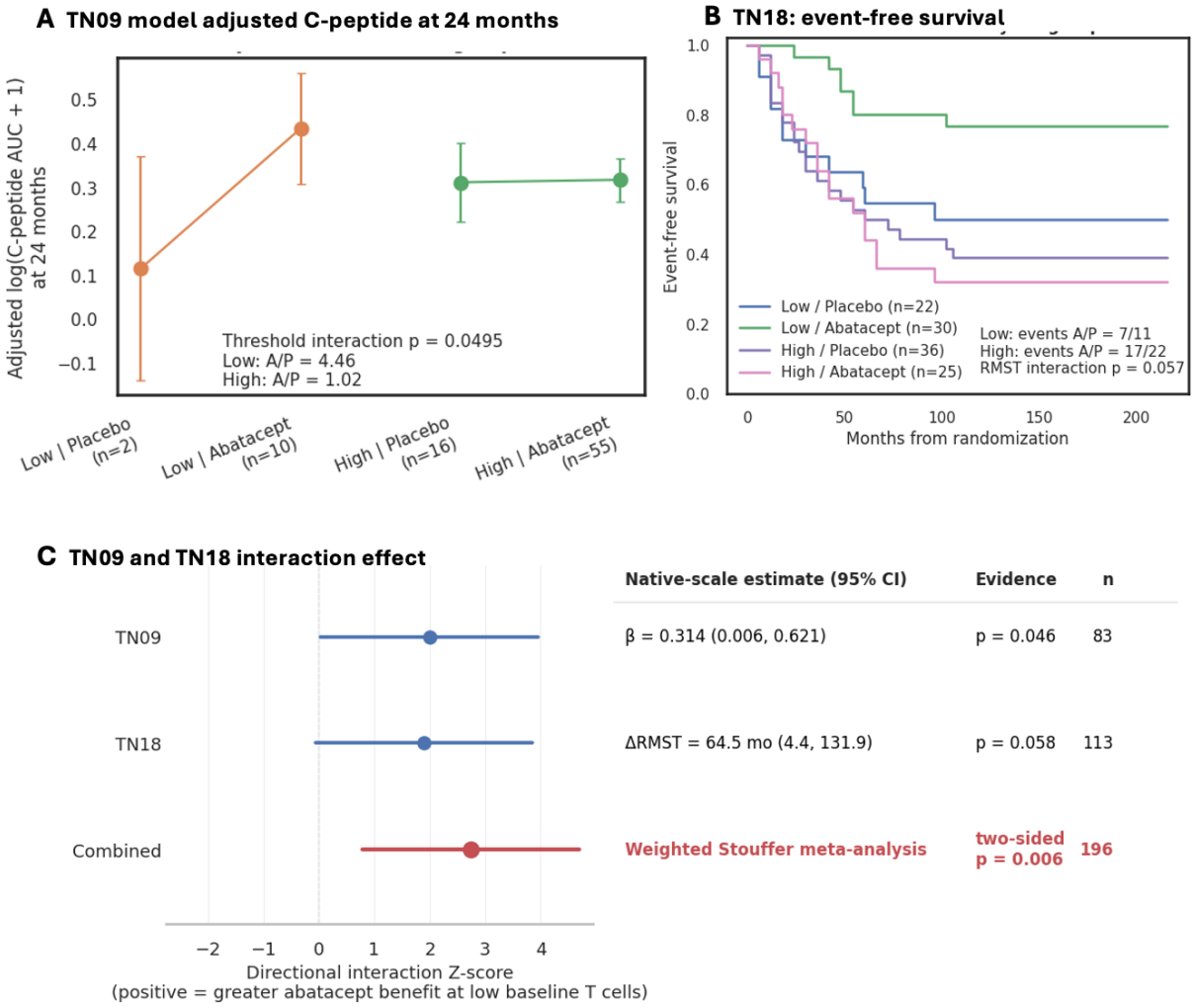


**Figure S8 | Baseline T-cell score is retrospectively associated with outcome heterogeneity in independent Abatacept studies**

A, TN09 treatment-by-subgroup interaction effect for 24-month C-peptide AUC, shown as the difference in abatacept-placebo separation between low and high baseline T-cell subgroups (beta = 0.413; 95% CI, 0.046 to 0.781; p = 0.0276; n = 61). B, TN18 directional interaction effect expressed as the difference in 96-month RMST benefit between low and high baseline T-cell subgroups (delta = 20.6 months; 95% CI, -3.3 to 45.2; permutation p = 0.0764; n = 83). C, Cross-trial aggregation of the directional interaction signal (weighted Stouffer Z = 2.78; one-sided p = 0.00271; two-sided p = 0.00541). D, TN09 model-adjusted mean 24-month C-peptide stratified by treatment and baseline T-cell subgroup; the treatment contrast is larger in the low-score subgroup than in the high-score subgroup (threshold-interaction p = 0.0319). E, TN18 event-free survival curves stratified by treatment and baseline T-cell subgroup; the low-score subgroup shows the larger favorable treatment separation (RMST interaction p = 0.085).

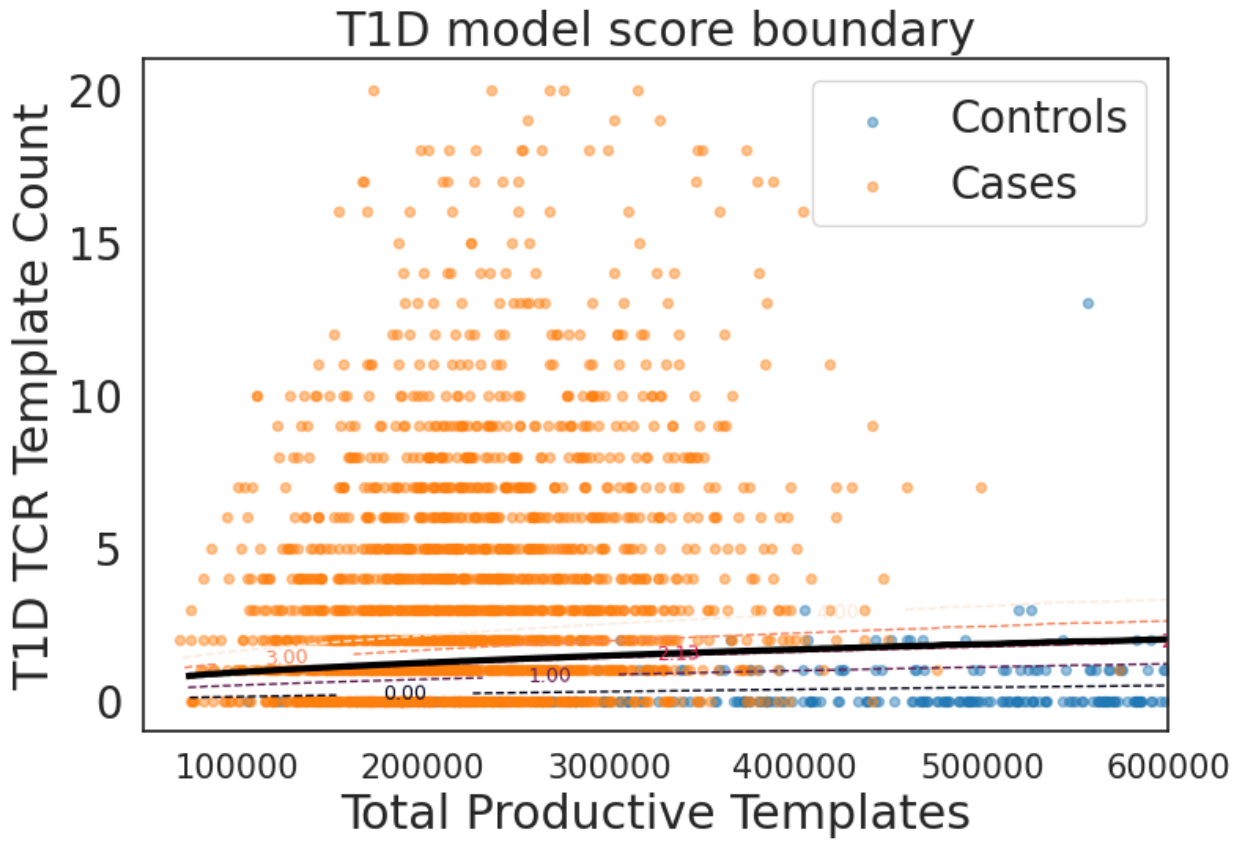


**Figure S9 | T1D Model Score ESLG model**

Each point is a sample in the training set. Orange represents cases and blue represents controls. Logistic growth curve fit to controls indicating 95% specificity cutoff is in black.

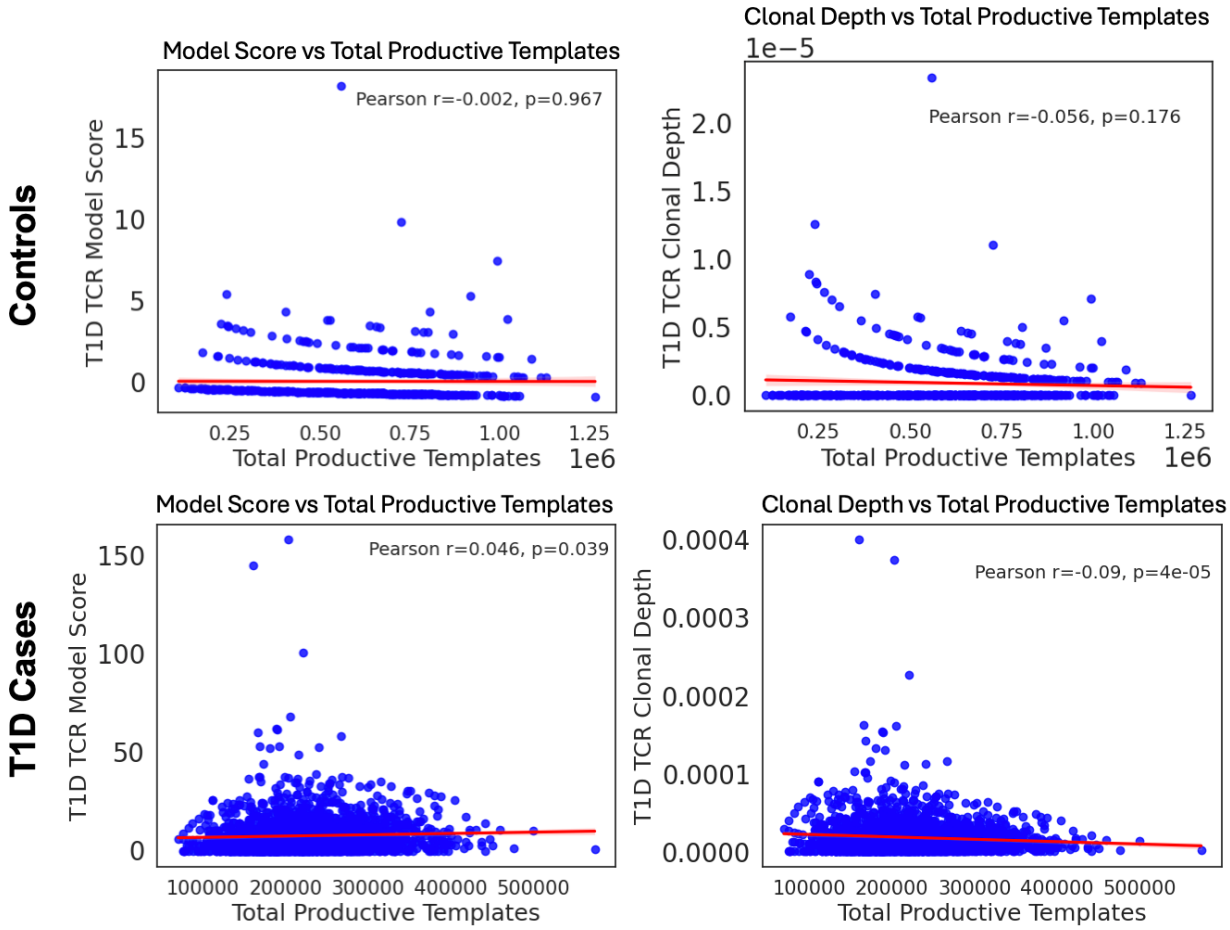


**Figure S10 | Correlation between model score and clonal depth vs productive templates**

The Z-score (model score) from the ESLG model has lower correlation with sequencing depth (productive templates) than clonal depth metric (model score r=0.056, clonal depth r=-0.09 in cases; model score r=-0.002, clonal depth r=-0.056 in controls).

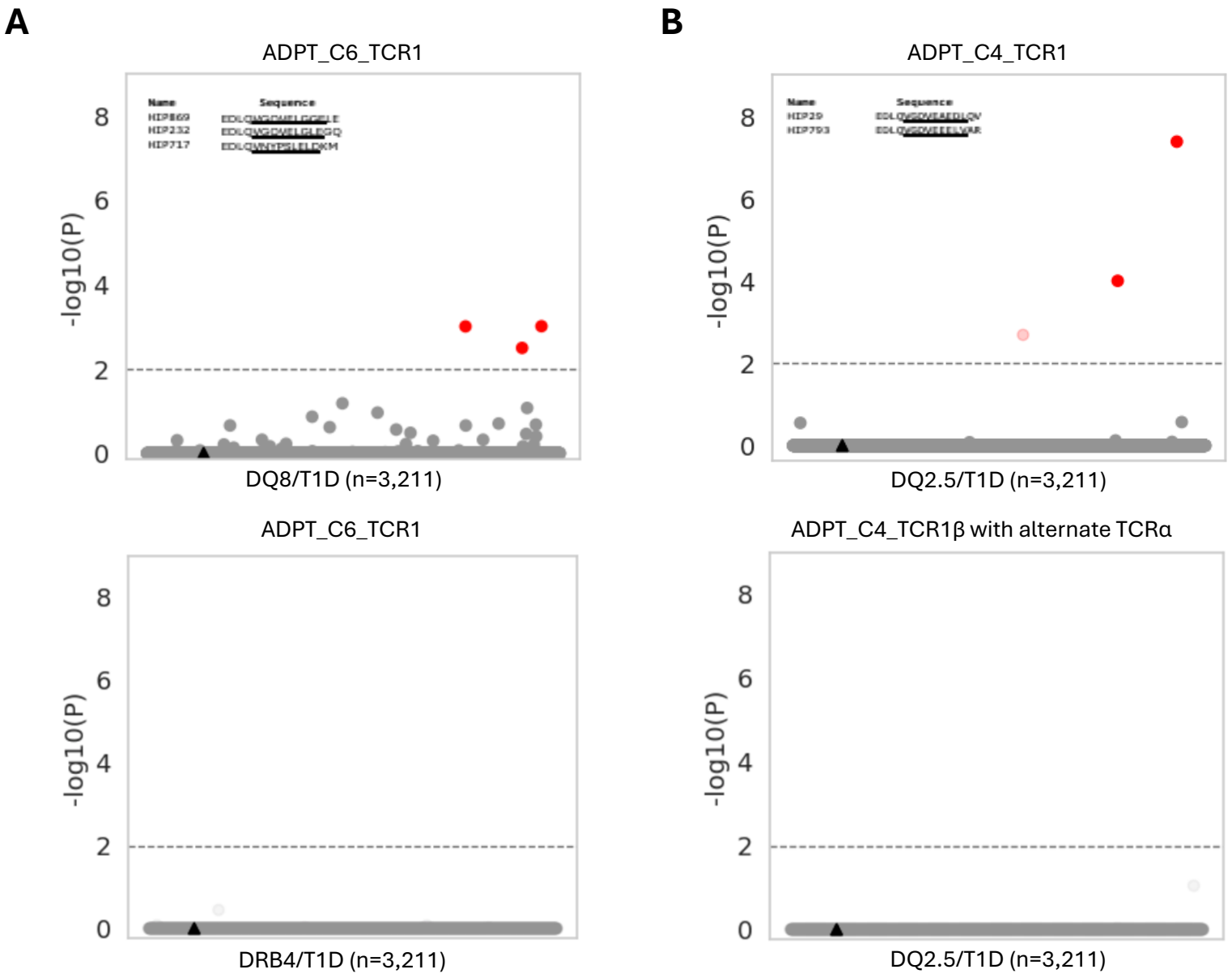


**Supplemental Figure 11. Antigen enrichment from the T1D library requires the correct HLA and TCRα.** Control experiments were performed to assess the importance of HLA restriction and TCRα subunit for antigen enrichment. **A**, An HLA-DQ8-restricted ADPT TCR (ADPT_C6_TCR1) enriched HIP sequences indicated in red from T1D library-expressing APrCs expressing HLA-DQ8 (Top) but not APrCs expressing a different HLA (HLA-DRB4; Below). **B**, An HLA-DQ2.5-restricted ADPT TCR (ADPT_C4_TCR1) enriched HIPs indicated in red from T1D library-expressing APrCs expressing HLA-DQ2.5 (Top; note same TCRαβ as Fig 5B center). None of the antigens are enriched when the TCRα is swapped for an alternate ((CAGTSNTGKLIF+V36-01+J37-01); Below). Significantly enriched HIP sequences are noted in each table. C-peptide is noted with a black triangle in each enrichment plot for reference.

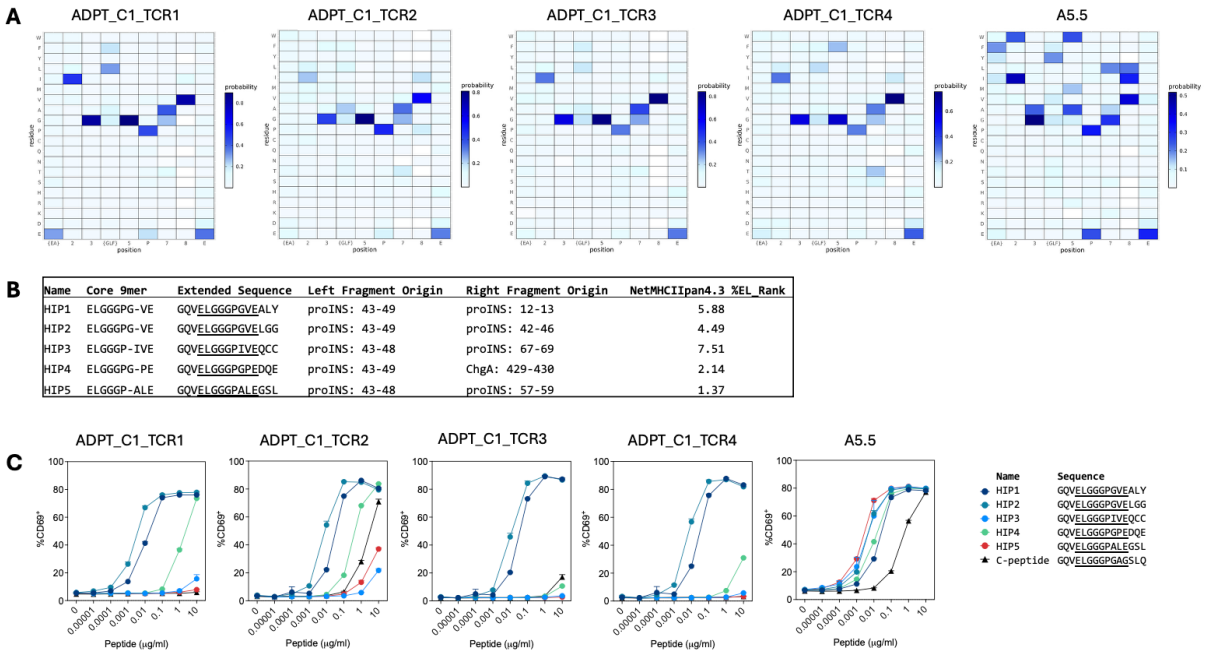


| Name | Core 9mer | Extended Sequence | Left Fragment Origin | Right Fragment Origin | NetMHCIIpan4.3 %EL_Rank |
|---|---|---|---|---|---|
| HIP1 | ELGGGPG-VE | GQVELGGGPGVEALY | proINS: 43-49 | proINS: 12-13 | 5.88 |
| HIP2 | ELGGGPG-VE | GQVELGGGPGVELGG | proINS: 43-49 | proINS: 42-46 | 4.49 |
| HIP3 | ELGGGP-IVE | GQVELGGGPIVEQCC | proINS: 43-48 | proINS: 67-69 | 7.51 |
| HIP4 | ELGGGPG-PE | GQVELGGGPGPEDQE | proINS: 43-49 | ChgA: 429-430 | 2.14 |
| HIP5 | ELGGGP-ALE | GQVELGGGPALEGSL | proINS: 43-48 | proINS: 57-59 | 1.37 |

**Supplemental Figure 12 | PS-SCL screening identifies HIP epitopes for TCRs from clusters ADPT_C1 and ADPT_C3.**

**A,** PS-SCL heatmaps are shown for five TCRs derived from two distinct TCR clusters. **B,** Reactivity profiles from PS-SCL screening were used to rank candidate HIP peptide sequences. The top five HIPs across all TCRs with a NetMHCIIpan-4.3 %EL_rank < 10 are displayed. The HIP junction is denoted by a hyphen, and the predicted 9-mer epitope is underlined. The origins of the N' terminal and C' terminal peptide fragments are indicated. An extended list of all HIPs identified by all five TCRs can be found in Supplementary Table S5a. **C,** T cell activation assays were used to assess TCR responsiveness to top-ranked HIPs. Dose-dependent peptide titration curves are shown, with activation quantified by CD69 upregulation.

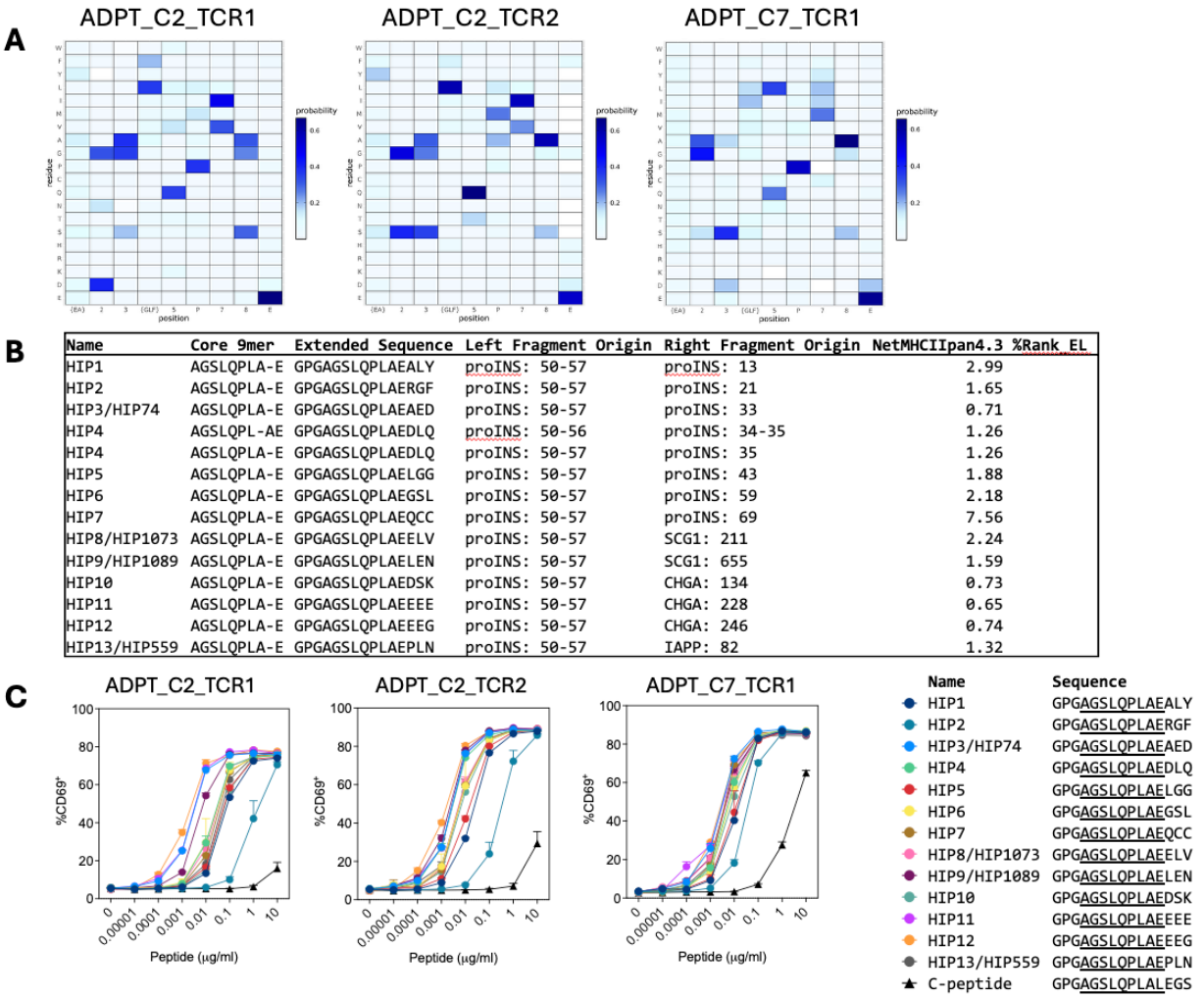


| Name | Core 9mer | Extended Sequence | Left Fragment Origin | Right Fragment Origin | NetMHCIIpan4.3 %Rank_EL |
|---|---|---|---|---|---|
| HIP1 | AGSLQPLA-E | GPGAGSLQPLAEALY | proINS: 50-57 | proINS: 13 | 2.99 |
| HIP2 | AGSLQPLA-E | GPGAGSLQPLAERGF | proINS: 50-57 | proINS: 21 | 1.65 |
| HIP3/HIP74 | AGSLQPLA-E | GPGAGSLQPLAEAED | proINS: 50-57 | proINS: 33 | 0.71 |
| HIP4 | AGSLQPL-AE | GPGAGSLQPLAEDLQ | proINS: 50-56 | proINS: 34-35 | 1.26 |
| HIP4 | AGSLQPLA-E | GPGAGSLQPLAEDLQ | proINS: 50-57 | proINS: 35 | 1.26 |
| HIP5 | AGSLQPLA-E | GPGAGSLQPLAELGG | proINS: 50-57 | proINS: 43 | 1.88 |
| HIP6 | AGSLQPLA-E | GPGAGSLQPLAEGSL | proINS: 50-57 | proINS: 59 | 2.18 |
| HIP7 | AGSLQPLA-E | GPGAGSLQPLAEQCC | proINS: 50-57 | proINS: 69 | 7.56 |
| HIP8/HIP1073 | AGSLQPLA-E | GPGAGSLQPLAEELV | proINS: 50-57 | SCG1: 211 | 2.24 |
| HIP9/HIP1089 | AGSLQPLA-E | GPGAGSLQPLAELEN | proINS: 50-57 | SCG1: 655 | 1.59 |
| HIP10 | AGSLQPLA-E | GPGAGSLQPLAEDSK | proINS: 50-57 | CHGA: 134 | 0.73 |
| HIP11 | AGSLQPLA-E | GPGAGSLQPLAEEEE | proINS: 50-57 | CHGA: 228 | 0.65 |
| HIP12 | AGSLQPLA-E | GPGAGSLQPLAEEEG | proINS: 50-57 | CHGA: 246 | 0.74 |
| HIP13/HIP559 | AGSLQPLA-E | GPGAGSLQPLAEPLN | proINS: 50-57 | IAPP: 82 | 1.32 |

**Supplemental Figure 13 | PS-SCL screening identifies HIP epitopes for TCRs from clusters ADPT_C2 and ADPT_C7.**

**A,** PS-SCL heatmaps are shown for three TCRs from two distinct TCR clusters. **B,** Reactivity profiles from PS-SCL screening were used to rank candidate HIP peptide sequences. The top 14 HIPs across all TCRs with a NetMHCIIpan-4.3 %EL_rank < 10 are displayed. The HIP junction is denoted by a hyphen, and the predicted 9-mer epitope is underlined. The origins of the N' terminal and C' terminal peptide fragments are indicated. An extended list of all HIPs identified by all three TCRs can be found in Supplementary Table S5b. **C,** T cell activation assays were used to assess TCR responsiveness to top-ranked HIPs. Dose-dependent peptide titration curves are shown, with activation quantified by CD69 upregulation.

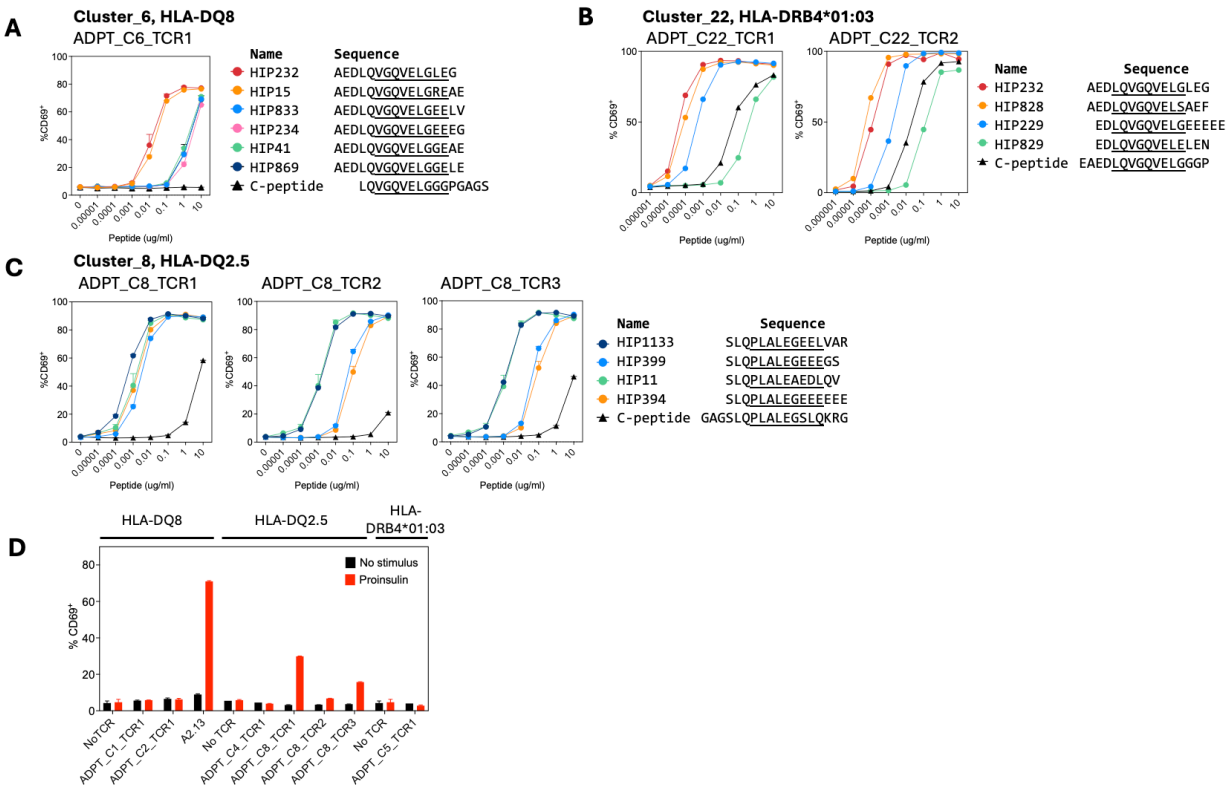


**Supplemental Figure 14 | Responsiveness of cluster_6, cluster_22 and cluster_8 TCRs to deorphanized HIPs and proinsulin.**

**A-C**, T cell activation assays assessing TCR responsiveness to top-ranked HIPs. Dose-dependent peptide titration curves are shown, with activation quantified by CD69 upregulation. **A,** ADPT_C6_TCR1 responses to VGQVELGxE-containing HIPs pulsed onto HLA-DQ8-expressing K562 cells. **B,** ADPT_C22_TCR1 and ADPT_C22_TCR2 responses to LQVGQVELx-containing HIPs pulsed onto HLA-DRB4*01:03-expressing K562 cells. **C,** ADPT_C8_TCR1, ADPT_C8_TCR2 and ADPT_C8_TCR3 responses to PLALExExx-containing HIPs pulsed onto HLA-DQ2.5-expressing K562 cells. **D,** T cell activation assay measuring responsivness of all TCRs to recombinant protein proinsulin at 50 µg/mL using K562 cells expressing the corresponding restricted HLA molecule.